PRESERVING ACCURATE MOTION CONTOURS WITH RELIABLE PARAMETER SELECTION

Javier Sánchez, Agustín Salgado and Nelson Monzón

Centro de Tecnologías de la Imagen (CTIM)
Department of Computer Science
University of Las Palmas de Gran Canaria
35017 Las Palmas de Gran Canaria, Spain

ABSTRACT

The use of decreasing functions, for mitigating the regularization at image contours, is typical in many recent optical flow methods. However, finding the correct parameter for getting the best of this strategy is challenging. Most of the methods use default parameters that are conservative, providing results that are not better than traditional approaches. Configurations that clearly enhance discontinuities may produce instabilities in the computed optical flows. This is due to the fact that the regularization process may get cancelled, yielding an *ill-posed* problem. In this work, we analyze the problem of instabilities and propose a method for efficiently determining the value of the parameter. We show that this approach allows us to obtain well preserved discontinuities at the same time that it avoids the *ill-posed* problem. The experiments with synthetic sequences demonstrate that the results are accurate and the selected parameter is close to the optimal value.

Index Terms— Optical Flow, Motion Estimation, Image Motion Analysis, Discontinuity-Preserving.

1. INTRODUCTION

The preservation of motion contours is a key problem in variational optical flow methods. Nowadays, there exist many strategies that yield accurate motion fields. In particular, the type of TV-L^1 approaches are ranked in the top of current benchmark databases. These methods succeed to produce piecewise smooth optical flows. However, they create rounded shapes near the borders of the objects and, normally, the edges do not coincide with image contours. These inconveniences occurs because the regularization process does not depend on the image information but only on the flow field itself.

In order to avoid these problems, many methods make use of decreasing functions to stop the regularization at object boundaries. This idea originally comes from [1] and has recently been used in many works, such as in [2, 3, 4, 5]. It is a simple solution and can certainly provide favorable results. Nevertheless, it has a strong dependency on the parameter of the decreasing function: if the parameter is underestimated, then the result is usually not better than basic TV approaches; on the other hand, if it is overestimated then it rapidly turns out to be unstable, providing poor results.

(a) (b) (c)

Fig. 1. From left to right: a) The first image of a sequence; b) the computed optical flow using decreasing functions; c) instabilities appearing around the object contours due to a wrong parameter value; and, at the bottom right corner of the third image, the color scheme used for motion representation.

Figure 1 depicts this situation. We see that this approach may yield good solutions if the parameter is properly chosen, as shown in the second image. Instabilities appear in the form of blobs around the object contour (third image), where the gradient of the image is large. In this case, a large value of the parameter has cancelled the smoothing behavior at high image gradients. The experimental results show that the plausible interval for the decay parameter is not very large in general, so its value must be chosen carefully. In many works, this parameter is given a default value, which is very conservative in practice [6].

The aim of this work is twofold. First, we study the effect of TV regularization at flow discontinuities. In particular, we analyze the use of decreasing functions and the reason for instabilities. Second, we deduce a mechanism for automatically computing the parameter value that avoids stopping the diffusion. This solves the ill-posed problem at the same time that it provides sharp discontinuities. The preservation of motion

This work has been partially supported by the Spanish Ministry of Science and Innovation through the research project TIN2011-25488 and the University of Las Palmas de Gran Canaria grant ULPGC011-006.

boundaries rely on the regularization parameter, the gradient of the flow and the gradient of the image. Instabilities appear when the regularization parameter is too small or when the gradient of the image is high. Our proposal depends on these elements to compute an efficient value.

In the experiments, we show that our approach typically yields nearly optimal solutions in real and synthetic sequences. For many sequences, the automatically selected parameter is close to the configuration that yields the best solution. For simple geometric sequences, discontinuities are clearly enhanced and the results are very accurate. In general, our proposal is interesting because it helps preserve sharp discontinuities, assures the stability of the results and is easy to implement.

Since the seminal work of Horn and Schunck [7], many works have appeared dealing with the problem of discontinuities. One of the former approaches is due to Nagel and Enkelman [8], who proposed a diffusion tensor for steering the regularization at image contours. Cohen [9], Proesmans *et al.* [10] and Black and Anandan [11], proposed anisotropic diffusion schemes based on TV regularization and robust statistics. Alvarez *et al.* [1] were the first to introduce an inhomogeneus scheme, based on decreasing functions, for inhibiting the smoothing at image contours. Later, in [12], the authors combined the Nagel-Enkelmann operator with a linear scale-space for dealing with contours and large displacements.

TV-L^1 approaches have been extensively used after the works of Brox *et al.* [13] and Zach *et al.* [14]. These two methods present the aforementioned problems about TV schemes, as shown in [15] and [16], respectively. Since then, many authors have combined TV regularizers with decreasing functions, like in [2, 3, 4, 5]. However, none of these approaches analyzes the mitigating scheme in depth. Even more, some of these use other mechanisms for enhancing the motion contours, so it is difficult to understand the influence of the decreasing function. Other alternatives propose to combine diffusion tensors and TV schemes, like in [17, 18]. The benefit of these strategies is that they are usually more stable, since the diffusion at discontinuities is never cancelled but oriented along the image contours. Nevertheless, these schemes do not completely stop the diffusion across the boundaries and, as a consequence, the motion discontinuities are normally smoothed. Other strategies, for enhancing discontinuities, rely on the estimation of the motion field using layers [19]. In [20], the authors proposed to use weighted median filters in a post-processing step, to refine the flow field at edges.

In Sect. 2, we introduce our optical flow model. Then, we minimize the energy functional in Sect. 2.1. In Sect. 2.2, we study the problem of instabilities and propose a global mechanism for automatically computing the parameter. The experimental results, in Sect. 3, analyze our proposal in depth, using synthetic geometric sequences and some sequences from the Middlebury benchmark database. Finally, a summary of the main ideas and conclusions in Sect. 4.

2. OPTICAL FLOW MODEL

Let $I_1, I_2 : \Omega \subset \mathbb{R}^2 \to \mathbb{R}$, be two consecutive images. The optical flow, $\mathbf{w} = (u(\mathbf{x}), v(\mathbf{x}))^T$, is a vector field that represents the displacement of the pixels from the first image into the second image. Our optical flow model relies on a global energy functional as follows:

$$\begin{aligned} E(\mathbf{w}) = &\int_\Omega \Psi\left(\left(I_2(\mathbf{x}+\mathbf{w}) - I_1(\mathbf{x})\right)^2\right) \mathbf{dx} \\ &+ \gamma \int_\Omega \Psi\left(\left|\nabla I_2(\mathbf{x}+\mathbf{w}) - \nabla I_1(\mathbf{x})\right|^2\right) \mathbf{dx} \\ &+ \alpha \int_\Omega \Psi\left(g(\nabla I_1)(|\nabla u|^2 + |\nabla v|^2)\right) \mathbf{dx}, \end{aligned} \quad (1)$$

with $\Psi(s^2) = \sqrt{s^2 + \epsilon^2}$ and $\epsilon := 0.001$ a small constant. $g(\nabla I_1) = e^{-\lambda|\nabla I_1|^\kappa}$ stands for a strictly decreasing function that inhibits regularization at object contours. In [6], the authors study its behavior with respect to λ and κ and conclude that $\kappa := 1$ is a good compromise between stability and accuracy, so we fix this parameter in the experiments.

2.1. Minimizing the energy functional

The minimum of (1) can be found by solving the associated Euler-Lagrange equations, given by

$$\begin{aligned} 0 = &\Psi'_d \cdot (I_2(\mathbf{x}+\mathbf{w}) - I_1(\mathbf{x})) \cdot I_{2,x}(\mathbf{x}+\mathbf{w}) \\ &+ \gamma\, \Psi'_g \cdot ((I_{2,x}(\mathbf{x}+\mathbf{w}) - I_{1,x}(\mathbf{x})) \cdot I_{2,xx}(\mathbf{x}+\mathbf{w}) \\ &+ (I_{2,y}(\mathbf{x}+\mathbf{w}) - I_{1,y}(\mathbf{x})) \cdot I_{2,xy}(\mathbf{x}+\mathbf{w})) \\ &- \alpha \operatorname{div}(\Psi'_s \cdot \nabla u), \\ 0 = &\Psi'_d \cdot (I_2(\mathbf{x}+\mathbf{w}) - I_1(\mathbf{x})) \cdot I_{2,y}(\mathbf{x}+\mathbf{w}) \\ &+ \gamma\, \Psi'_g \cdot ((I_{2,x}(\mathbf{x}+\mathbf{w}) - I_{1,x}(\mathbf{x})) \cdot I_{2,xy}(\mathbf{x}+\mathbf{w}) \\ &+ (I_{2,y}(\mathbf{x}+\mathbf{w}) - I_{1,y}(\mathbf{x})) \cdot I_{2,yy}(\mathbf{x}+\mathbf{w})) \\ &- \alpha \operatorname{div}(\Psi'_s \cdot \nabla v), \end{aligned} \quad (2)$$

with $\Psi'_d := \Psi'((I_2(\mathbf{x}+\mathbf{w}) - I_1(\mathbf{x}))^2)$, $\Psi'_g := \Psi'(|\nabla I_2(\mathbf{x}+\mathbf{w}) - \nabla I_1(\mathbf{x})|^2)$ and $\Psi'_s := \Psi'(e^{-\lambda|\nabla I_1|}(|\nabla u|^2 + |\nabla v|^2))$.

In order to solve this system, we discretize the equations using centered finite differences. Then, the system of equations is solved by means of an iterative approximation, such as the SOR method. Due to the nonlinear nature of these formulas, the resolution of these equations requires two fixed point iterations. The warpings of I_2 are approximated using Taylor expansions and bicubic interpolation. We also use a multiscale strategy for recovering large displacements. Starting from the coarsest scales, we obtain a solution and then upgrade the value of the optical flow for the next finer scale.

We use *motion increments*, $\mathbf{w}^{k+1} = \mathbf{w}^k + \mathbf{dw}^k$, so that, in each scale, we compute each increment, $\mathbf{dw}^k$. The final optical flow is obtained as an accumulative value for all increments. More details about the implementation of this scheme are given in [13, 15].

2.2. Ill-posedness of the inhomogeneous model

The smoothing term in (2) is given by $S(u) = \alpha \operatorname{div}(\Psi'_s \cdot \nabla u)$ and $S(v) = \alpha \operatorname{div}(\Psi'_s \cdot \nabla v)$. Then, the diffusivity, including α, is

$$\mathcal{D}(\mathbf{x}) = \frac{\alpha e^{-\lambda|\nabla I_1|}}{\sqrt{e^{-\lambda|\nabla I_1|}\left|\nabla \mathbf{w}\right|^2 + \epsilon^2}}. \tag{3}$$

with $\left|\nabla \mathbf{w}\right|^2 = \left|\nabla u\right|^2 + \left|\nabla v\right|^2$. The *ill-posed* problem appears when this diffusivity becomes zero. This is equivalent to cancel the regularization term in the energy functional (1). Thus, this problem may arise when λ or ∇I_1 are very large, or α is too small.

In order to circumvent this problem, we may assure a minimum isotropic regularization as follows: Let $\mathcal{D}(\mathbf{x}) = \xi$, with ξ a small constant, e.g., $\xi := 1 \times 10^{-3}$, then, solving for λ, we obtain two solutions

$$\lambda_{1,2} = -\ln\left(\xi \frac{\left|\nabla \mathbf{w}\right|^2 \xi \pm \sqrt{\left(\left|\nabla \mathbf{w}\right|^2\right)^2 \xi^2 + 4\alpha^2\epsilon^2}}{2\alpha^2 \left|\nabla I_1\right|}\right), \tag{4}$$

one real and another imaginary, which can be discarded.

If we analyze further, we find that the denominator of (3) is bounded in the limits

$$0 < \sqrt{e^{-\lambda|\nabla I_1|}\left|\nabla \mathbf{w}\right|^2 + \epsilon^2} \leq \sqrt{\left|\nabla \mathbf{w}\right|^2 + \epsilon^2} \approx \left|\nabla \mathbf{w}\right|, \tag{5}$$

with the upper bound approximately equal to the flow magnitude. In this sense, the denominator does not pose any problem because it will never be very large: in practical situations, the magnitude of the flow will be much smaller than the image size. The main problem emerges when $\alpha e^{-\lambda|\nabla I_1|} \cong 0$. We avoid this situation imposing the following constraint

$$\alpha e^{-\lambda|\nabla I_1|} = \xi. \tag{6}$$

Solving for λ we obtain

$$\lambda = \frac{-\ln(\xi) + \ln(\alpha)}{\left|\nabla I_1\right|}. \tag{7}$$

ξ must be chosen so that the diffusivity is large enough to avoid the ill-posedness. Notice that, in (4) and (7), λ must be a function of $\mathbf{x}$, the same as ∇I_1 and $\nabla \mathbf{w}$.

Determining the value of λ. We propose a global approach for determining a unique value for λ. For this, we can search the minimum value that satisfies one of the following conditions:

$$\left(\frac{\alpha e^{-\lambda|\nabla I_1|}}{\sqrt{e^{-\lambda|\nabla I|}\left|\nabla \mathbf{w}\right|^2 + \epsilon^2}} \geq \xi\right) \quad \text{or} \quad \left(\alpha e^{-\lambda|\nabla I_1|} \geq \xi\right), \tag{8}$$

taking into account (3) or (6), respectively. Selecting the second condition for simplicity, the maximum gradient of the image yields the minimum value as

$$\lambda_g := \frac{-\ln(\xi) + \ln(\alpha)}{\max\limits_{\mathbf{x}\in\Omega}\{|\nabla I_1(\mathbf{x})|\}}. \tag{9}$$

This will provide a unique value, which is obtained from the more restrictive situation. The advantage of this approach is that it automatically obtains λ and eliminates the instability problems, as seen in Fig. 1. In the experimental results, we will see that this value is nearly optimal in many cases, correctly preserving the discontinuities of the flow.

3. EXPERIMENTAL RESULTS

In this section, we analyze the influence of the decreasing function. Most of the parameters are set according to [15], except α and λ that are adapted in each experiment. We use two datasets: one with geometric figures, presenting pronounced discontinuities and large displacements; and some sequences from the Middlebury benchmark database [21].

Figure 2 shows several results using the *Brox et al.* method and $g = e^{-\lambda_g|\nabla I_1|}$, with λ_g defined in (9). For the Geometric sequences, the *Brox et al.* method cannot completely stop the diffusion at discontinuities. We can see that it has many difficulties to deal with this type of figures: it creates rounded contours; motion edges are clearly dislocated from the object boundaries; it cannot separate the motion of close figures, like in the two rectangles sequence; and the motion is severely affected by occlusions.

On the other hand, the exponential function allows to solve these problems. We observe that the solutions are very similar to the ground truths, providing very good accuracies. It can even deal with occlusions in the Geometric sequences. This is an interesting behavior since we have not included any mechanism for handling occlusions. For this, we have sufficiently increased the value of the regularization parameter so that the smoothing term outweighs the attachment to the intensity information. Although the Geometric sequences are very simple, the solutions show us the possibilities of this approach.

Looking at the results on the Middlebury dataset, we observe that the *Brox et al.* method presents the same shortcomings as in the previous experiments. However, the computed flow fields with the exponential function are very promising. The preservation of flow discontinuities is evident in the last column. Nevertheless, the occlusion problem has not been

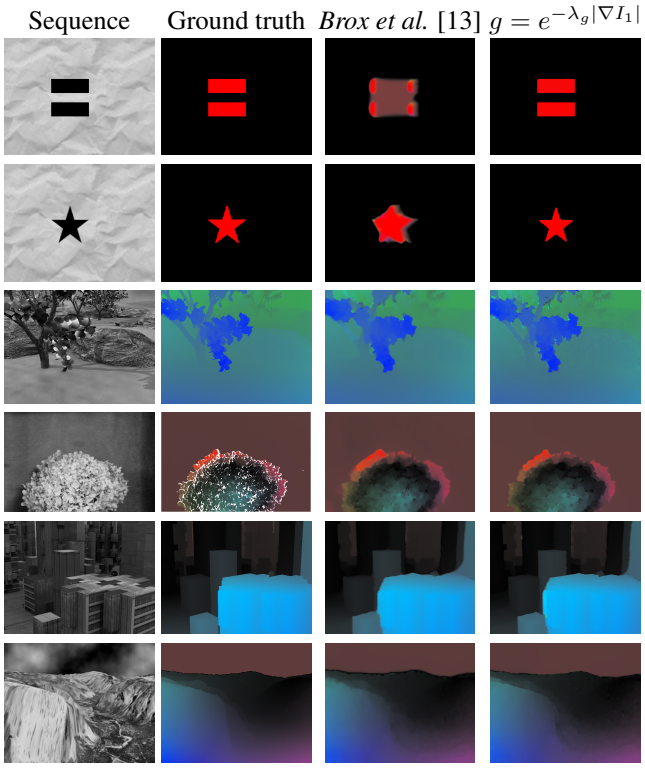

Fig. 2. Results for the Geometric and Middlebury sequences. Left column, the first image; second, the corresponding ground truth; third, results using the *Brox et al.* [13] method; and, fourth, results with our proposal.

solved as before. In this case, we have chosen smaller regularization parameters to avoid over-smoothing the vector fields. In *Hydrangea*, *Urban2* and *Yosemite with clouds*, the motion boundaries are very similar to the ground truth, except at occlusions. For instance, in the last sequence, there is a clear separation between the motion corresponding to the clouds and the mountains. It even detects the contour of some mountains with high precision.

Figure 3 shows the Average Angular Error (AAE) evolution with respect to λ. We observe that the use of the decreasing function (blue line) allows improving the result of the *Brox et al.* method ($\lambda := 0$). In the case of the Geometric sequences, the improvement is very important, achieving low error measures. For the Middlebury sequences, the improvement is also interesting but, in some cases, moderate. After reaching the minimum value, the errors in the exponential graphics quickly grow. It turns unstable for larger values of λ. From this point, the blobs seen in Fig. 1 start to appear in the computed optical flows.

From these graphics, we may conclude that the use of decreasing functions is interesting for preserving discontinuities only if the parameters are carefully chosen. Otherwise, the method provides worse results than the *Brox et al.* approach and may turn unstable. Interestingly, our proposal for computing the parameter yields very good results. The red line is the solution obtained with λ_g, which is automatically calculated in (9). The green dot is the value obtained with this formula. We can see that most of the solutions are near the minimum of the exponential graphics, thus providing a nearly optimal value.

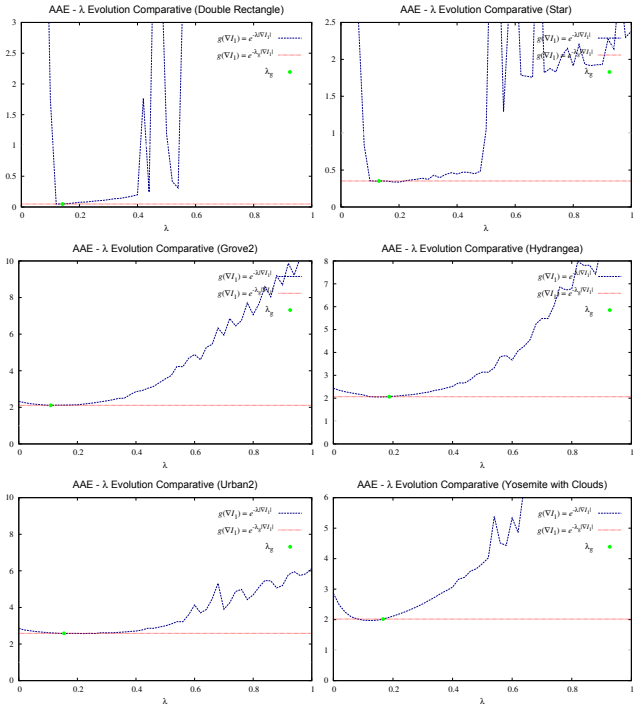

Fig. 3. Average Angular Error (AAE) evolution with respect to λ for the Geometric and Middlebury sequences.

4. CONCLUSION

In this work, we demonstrated that the use of decreasing functions solves many of the TV-L^1 shortcomings: it allows to preserve motion contours and clearly separate different moving regions; in general, the flow boundaries coincide with image edges; it also allows dealing with occlusions; and it provides high accuracy in simple geometric sequences, where basic TV approaches have severe difficulties. We have seen that the selection of the parameter is critical for obtaining good solutions: small values may yield results which are not better than traditional methods and large values clearly worsen the results, creating instabilities in the flow field. We proposed an automated mechanism for determining the value that assures a minimum isotropic smoothing. In the experimental results we saw that our proposal provided very good results. It avoids instabilities and produces values which are typically near the optimal parameter.

5. REFERENCES

[1] Luis Alvarez, Julio Esclarín, Martin Lefébure, and Javier Sánchez, "A PDE model for computing the optical flow," in *XVI Congreso de Ecuaciones Diferenciales y Aplicaciones (CEDYA)*, Las Palmas de Gran Canaria, Spain, 1999, pp. 1349–1356.

[2] Andreas Wedel, Daniel Cremers, Thomas Pock, and Horst Bischof, "Structure- and motion-adaptive regularization for high accuracy optic flow," in *Proceedings of IEEE International Conference on Computer Vision*, Sept. 2009, pp. 1663–1668.

[3] Li Xu, Jiaya Jia, and Yasuyuki Matsushita, "Motion detail preserving optical flow estimation," *IEEE Transactions on Pattern Analysis and Machine Intelligence*, vol. 34, no. 9, pp. 1744–1757, Sept. 2012.

[4] Zhuoyuan Chen, Hailin Jin, Zhe Lin, Scott Cohen, and Ying Wu, "Large displacement optical flow from nearest neighbor fields," in *Computer Vision and Pattern Recognition (CVPR)*. 2013, pp. 2443–2450, IEEE Computer Society.

[5] Tae Hyun Kim, Heeseok Lee, and Kyoung Mu Lee, "Optical flow via locally adaptive fusion of complementary data costs," in *International Conference on Computer Vision (ICCV)*. 2013, IEEE Computer Society.

[6] Nelson Monzón, Javier Sánchez, and Agustín Salgado, "Optic flow: Improving discontinuity preserving," in *14th International Conference on Computer Aided Systems Theory (EUROCAST)*, Berlin, Heidelberg, 2013, pp. 114–116, Springer-Verlag.

[7] Berthold K. P. Horn and Brian G. Schunck, "Determining optical flow," *Artificial Intelligence*, vol. 17, pp. 185–203, 1981.

[8] Hans-Helmut Nagel and Wilfried Enkelmann, "An investigation of smoothness constraints for the estimation of displacement vector fields from image sequences," *IEEE Transanctions on Pattern Analysis and Machine Intelligence*, vol. 8, pp. 565–593, September 1986.

[9] Isaac Cohen, "Nonlinear Variational Method for Optical Flow Computation," in *Proceedings of the 8th Scandinavian Conference on Image Analysis*, Tromso, Norway, 1993, IAPR, pp. 523–530.

[10] Marc Proesmans, Luc Van Gool, Eric Pauwels, and André Oosterlinck, "Determination of optical flow and its discontinuities using non-linear diffusion," in *third European Conference on Computer Vision*, Secaucus, NJ, USA, 1994, vol. 2, pp. 295–304, Springer-Verlag.

[11] Michael J. Black and P. Anandan, "A framework for the robust estimation of optical flow," in *Proceedings of Fourth International Conference on Computer Vision*, 1993, pp. 231–236.

[12] Luis Alvarez, Joachim Weickert, and Javier Sánchez, "Reliable estimation of dense optical flow fields with large displacements," *International Journal of Computer Vision*, vol. 39, no. 1, pp. 41–56, 2000.

[13] Thomas Brox, Andrés Bruhn, Nils Papenberg, and Joachim Weickert, "High accuracy optical flow estimation based on a theory for warping," in *European Conference on Computer Vision (ECCV)*, Prague, Czech Republic, May 2004, vol. 3024 of *LNCS*, pp. 25–36, Springer.

[14] Christopher Zach, Thomas Pock, and Horst Bischof, "A Duality Based Approach for Realtime TV-L1 Optical Flow," in *Pattern Recognition*, vol. 4713 of *Lecture Notes in Computer Science*, chapter 22, pp. 214–223. Springer Berlin Heidelberg, Berlin, Heidelberg, 2007.

[15] Javier Sánchez, Nelson Monzón, and Agustín Salgado, "Robust optical flow estimation," *IPOL: Image Processing Online*, vol. Preprint, pp. 1–18, 2012.

[16] Javier Sánchez, Enric Meinhardt-Llopis, and Gabriele Facciolo, "TV-L1 Optical Flow Estimation," *Image Processing On Line*, vol. 2013, pp. 137–150, 2013.

[17] Manuel Werlberger, Werner Trobin, Thomas Pock, Andreas Wedel, Daniel Cremers, and Horst Bischof, "Anisotropic huber-l1 optical flow," in *Proceedings of the British Machine Vision Conference (BMVC)*, London, UK, September 2009, to appear.

[18] Henning Zimmer, Andrés Bruhn, and Joachim Weickert, "Optic flow in harmony," *International Journal of Computer Vision*, vol. 93, no. 3, pp. 368–388, July 2011.

[19] Deqing Sun, E. Sudderth, and Michael J. Black, "Layered Image Motion with Explicit Occlusions, Temporal Consistency, and Depth Ordering," in *Advances in Neural Information Processing Systems 23*, 2010, vol. 23, pp. 2226–2234.

[20] Deqing Sun, Stefan Roth, and Michael J. Black, "Secrets of optical flow estimation and their principles," in *IEEE Conference on Computer Vision and Pattern Recognition*, Los Alamitos, CA, USA, 2010, pp. 2432–2439, IEEE Computer Society.

[21] Simon Baker, Daniel Scharstein, J. P. Lewis, Stefan Roth, Michael J. Black, and Richard Szeliski, "A database and evaluation methodology for optical flow," in *International Conference on Computer Vision*, 2007, pp. 1–8.